Dipolar spin-wave modes of a ferromagnetic multilayer with alternating directions of magnetization

K. Mika and P. Grünberg
Institut für Festkörperforschung, Kernforschungsanlage Jülich GmbH, D-5170 Jülich, West Germany
(Received 22 October 1984)

The spin-wave spectrum of a ferromagnetic multilayer with alternating directions of magnetization is derived in the dipolar magnetostatic limit. The external magnetic field is set equal to zero and the magnetization is assumed to be in-plane but reversed in adjacent films. We find interesting qualitative differences for an even and an odd number N of single layers which constitute the multilayer. The solutions can be classified as bulklike or surfacelike with respect to the whole multilayer. As $N \rightarrow \infty$ the bulklike solutions form bands. We also discuss some symmetry aspects of these solutions.

I. INTRODUCTION

Mode spectra of ferromagnetic multilayers have recently become of increased interest both in basic research[1–4] and also for application in microwave devices.[5] It appears that the spectrum of coupled multilayer modes is the only true collective magnetic phenomenon of multilayers. All other features which have been found up to now can be explained in terms of modified single-film properties. From the application point of view, having a multilayer instead of a single film obviously offers more degrees of freedom for tailoring special properties. Another way to do this, for example, is combining the magnetic layer in some way with a nonmagnetic metallic layer which has a strong effect on the electric fields associated with these modes. On the other hand, when using a multilayer, variation of the number of layers or their thickness does not yet exhaust the number of possibilities. One could consider, for example, choosing different magnetizations for different films composing a multilayer or in particular having the direction of the magnetization reversed in adjacent films. With this possibility in mind we have found it worthwhile to extend previous work on ferromagnetic multilayers[2] with parallel magnetization to the case of antiparallel alignment between neighboring films. We call this in the following an "antiparallel multilayer" (APML) (see Fig. 1).

Another motivation for us to look into this problem was given by some aspects of spatial symmetry which should have an effect on the kind of solutions one obtains. As will be seen, these aspects are of more interest in the case of the antiparallel multilayer as compared to the parallel one. In particular there is an important difference whether the multilayer contains an even or an odd number of single layers. These symmetries exist only in zero external magnetic field B_0. If one would like to investigate such a system experimentally, B_0 equal to zero or at least small B_0 would also be necessary because otherwise the films would align all parallel to the external field. The antiparallel alignment could for example be achieved by fabrication of a multilayer with films of alternating coercive forces. This is possible by choosing the proper evaporation conditions. The situation would be particularly clear if we had rectangular hysteresis curves on all films. Suppose now the multilayer consists of one set of films with a large coercive force interpenetrated by another set with a smaller one. If we saturate all films in due direction with a large enough field and then scan the field through zero up to the smaller coercive field in the opposite direction, the corresponding set of films would reverse its magnetization whereas the other set would stay in the initial state. The result would be an APML. If the hysteresis curves are rectangular, this situation will not change by now reducing the external field to zero. This is the situation for which we want to derive in the following the mode spectrum. As in Ref. 2 we restrict ourselves to transverse propagation of the modes, along the y axis in Fig. 1.

Another way of getting an APML of course would be by having a negative exchange interaction of the ferromagnetic films across the interlayers. For positive ex-

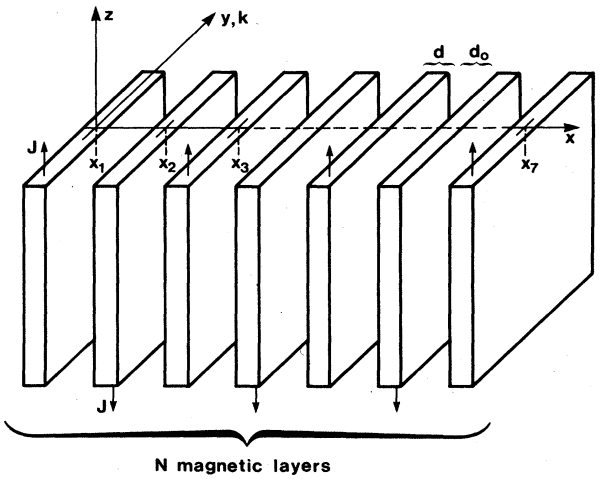

FIG. 1. Antiparallel multilayer. There are N (here $N=7$) magnetic layers of thickness d separated by a distance d_0. We assume infinite extent in the $\pm y, \pm z$ directions. External field is zero. Direction of the magnetization J is alternating.

change this has recently been investigated experimentally,[6] although the origin of the effect is still somewhat unclear. Neither positive nor negative interlayer exchange has so far been discussed theoretically and we will not discuss this either. Here as mentioned the APML is thought to exist due to particular hysteresis effects. We will discuss the inclusion of a negative interlayer exchange and the relation between an APML and an antiferromagnet (AF) briefly in the final section.

II. MODE FREQUENCIES

Apart from now having the antiparallel alignment, the procedure of setting up the equations for the mathematical treatment of our problem is exactly the same as in Ref. 2 for the parallel multilayer. Since we want to use the same abbreviations it is not necessary to repeat them here.

From the equations (2.2)–(2.5) of Ref. 2, which were derived for the parallel case, we obtain those for the antiparallel case in the following way. First, since the external field is now supposed to be zero, the quantity κ by definition is also zero. Second, in the prefactors of the coefficients g_l,h_l we have to replace ν by $-\nu$ when g_l,h_l belongs to a film with reversed magnetization.

The system of $2N-2$ Eqs. (2.2) of Ref. 2 can then be put into the following form:

$$\begin{aligned} &m_1 g_{2l-1}+m_2 h_{2l-1}+m_3 g_{2l}+m_4 h_{2l}=0 ,\\ &m_5 g_{2l-1}+m_6 h_{2l-1}+m_7 g_{2l}+m_8 h_{2l}=0 ,\\ &\overline{m}_1 g_{2l}+\overline{m}_2 h_{2l}+\overline{m}_3 g_{2l+1}+\overline{m}_4 h_{2l+1}=0 ,\\ &\overline{m}_5 g_{2l}+\overline{m}_6 h_{2l}+\overline{m}_7 g_{2l+1}+\overline{m}_8 h_{2l+1}=0 , \end{aligned} \tag{2.1}$$

for $l=1,\ldots,L$. This system ends with the first two equations if $N=2L$, and with the second pair of equations if $N=2L+1$, and N is defined in Fig. 1. Here

$$\begin{aligned} &m_1=(1+\lambda)e^{kd}, \quad m_2=1 ,\\ &m_3=(1-\lambda)e^{-kd_0}, \quad m_4=e^{k(d-d_0)} ,\\ &m_5=e^{kd}, \quad m_6=1-\lambda ,\\ &m_7=e^{kd_0}, \quad m_8=(1+\lambda)e^{k(d+d_0)} , \end{aligned} \tag{2.2}$$

and $\overline{m}_i(\lambda)=m_i(-\lambda)$, $i=1,\ldots,8$, where we have set $\lambda=2/\nu$.

We complete this set of equations for the $2N$ coefficients g_l,h_l by adding the two equations

$$g_1+(1-\lambda)e^{kd}h_1=0 , \tag{2.3a}$$

$$[1-(-1)^N\lambda]e^{kd}g_N+h_N=0 , \tag{2.3b}$$

which correspond to Eq. (2.4) of Ref. 2.

Equations (2.1) and (2.3) form a homogeneous system $Mx=0$ with nontrivial solutions x, if the determinant of M vanishes, which then determines λ. Since λ enters linearly into the elements m_{ij} of M, we can also write

$$M_1 x=\lambda M_2 x , \tag{2.4}$$

where M_1,M_2 are independent of λ. This is therefore a generalized eigenvalue problem and the λ_n are the eigenvalues of $M_2^{-1}M_1$.

For later purposes it is more convenient to modify the system (2.1) slightly by multiplying the second and fourth equation by $\exp(-kd_0)$. We then have $m_5=m_4$, $m_6=m_3$, $m_7=m_2$, $m_8=m_1$, and (2.1) becomes

$$\begin{aligned} &Av_{2l-1}+Bv_{2l}=0 ,\\ &Cv_{2l}+Dv_{2l+1}=0 , \end{aligned} \tag{2.5}$$

with

$$\begin{aligned} A&=\begin{bmatrix} (1+\lambda)e^{kd} & 1 \\ e^{k(d-d_0)} & (1-\lambda)e^{-kd_0} \end{bmatrix} ,\\ B&=\begin{bmatrix} (1-\lambda)e^{-kd_0} & e^{k(d-d_0)} \\ 1 & (1+\lambda)e^{kd} \end{bmatrix} ,\\ C&=\begin{bmatrix} (1-\lambda)e^{kd} & 1 \\ e^{k(d-d_0)} & (1+\lambda)e^{-kd_0} \end{bmatrix} ,\\ D&=\begin{bmatrix} (1+\lambda)e^{-kd_0} & e^{k(d-d_0)} \\ 1 & (1-\lambda)e^{kd} \end{bmatrix} , \end{aligned} \tag{2.6}$$

and v_l equals the transpose of (g_l,h_l).

We want to solve the system (2.5) recursively. We introduce the matrix

$$E=D^{-1}CB^{-1}A \tag{2.7}$$

and obtain

$$v_{2l+1}=Ev_{2l-1} , \tag{2.8}$$

or

$$v_{2l+1}=E^l v_1 . \tag{2.9}$$

The corresponding expression for v_{2l+2} is

$$v_{2l+2}=-B^{-1}AE^l v_1 . \tag{2.10}$$

It is therefore obvious that the eigenvalues of E will be important for the characterization of the modes λ_n, especially for large N.

The elements of E are

$$e_{11}=e^{2k(d_0+d)}+2\lambda^{-2}[1-e^{2k(d_0+d)}-e^{2kd}+\cosh(2kd_0)]+\lambda^{-4}[e^{2k(d_0+d)}+2(1-e^{2kd})+e^{-2k(d_0-d)}-2\cosh(2kd_0)] , \tag{2.11a}$$

$$e_{12}=2\lambda^{-1}\{\sinh[k(2d_0+d)]+\sinh(kd)\}-2\lambda^{-2}\{\sinh[k(2d_0+d)]+3\sinh(kd)\} -2\lambda^{-4}(\lambda-1)\{\sinh[k(2d_0+d)]-2\sinh(kd)-\sinh[k(2d_0-d)]\} , \tag{2.11b}$$

$$e_{21}(\lambda)=-e_{12}(-\lambda) , \tag{2.11c}$$

$$e_{22}(k)=e_{11}(-k) , \tag{2.11d}$$

and the eigenvalues of E are

$$\rho_{1,2}=\alpha\pm(\alpha^2-1)^{1/2}\ , \tag{2.12}$$

with

$$\alpha=\mu_2+2\lambda^{-2}\mu_1+2\lambda^{-4}\mu_0\ , \tag{2.13}$$

and

$$\begin{aligned}\mu_0&=[\cosh(2kd)-1][\cosh(2kd_0)-1]\ ,\\ \mu_1&=1-\cosh(2kd)+\cosh(2kd_0)\\ &\quad-\cosh[2k(d_0+d)]\ ,\\ \mu_2&=\cosh[2k(d_0+d)]\ .\end{aligned} \tag{2.14}$$

As in Ref. 2, we distinguish between the two cases where ρ_1 and ρ_2 are complex or real.

A. Case 1

ρ_1 and ρ_2 are complex. This occurs for (real) values of λ if $|\alpha|<1$. From (2.12) follows that $\rho_1\rho_2=1$. With $\rho_2=\rho_1^*$ we can therefore write $\rho_1=\exp(i\phi)$, $\rho_2=\exp(-i\phi)$, where ϕ is a function of λ. The values of λ are determined by Eq. (2.3b) which contains g_N and h_N. Now g_N,h_N depend on $\rho_{1,2}$ [see, e.g., Eq. (2.20) below]. Due to the oscillatory behavior of $\rho_{1,2}$, the solutions λ_n form bands which become dense for $N\to\infty$.

The band edges follow from the condition $|\alpha|=1$, which according to (2.13) leads to

$$\lambda^2(\sigma,\tau)=\frac{1}{\mu_2+\sigma}\{-\mu_1+\tau[\mu_1^2-2\mu_0(\mu_2+\sigma)]^{1/2}\}\ ,$$
$$\sigma,\tau=\pm1\ . \tag{2.15}$$

We thus obtain four bands with lower and upper band edges $\lambda(-1,-1),\lambda(+1,-1)$ for the lower positive band, and $\lambda(+1,+1),\lambda(-1,+1)$ for the upper positive band, respectively.

For small d_0, the positive roots of (2.15) are

$$\lambda(-1,-1)=kd_0-(kd_0)^2\coth(kd)+O(d_0^3)\ , \tag{2.16a}$$
$$\lambda(+1,-1)=kd_0-(kd_0)^2\coth(kd)+O(d_0^3)\ , \tag{2.16b}$$
$$\lambda(+1,+1)=2\tanh(kd)+O(d_0)\ , \tag{2.16c}$$
$$\lambda(-1,+1)=2-(kd_0)\coth(kd)+O(d_0^2)\ , \tag{2.16d}$$

and for $d_0\to\infty$ we have

$$\lambda^2(\sigma,\tau)=1-e^{-2kd} \tag{2.17}$$

for all band edges. Figure 2 shows the positive eigenvalues λ_n together with the band edges as a function of d_0 for $N=41$. We observe a very narrow lower band, which is a consequence of (2.16a), (2.16b), and (2.17).

The result (2.16d) for the upper band edge of the upper positive band is quite remarkable because as it is now, it means that there is a finite frequency for $k=0$ and $B_0=0$. However, this is only true in the limit of $N\to\infty$. For finite N (and finite d) all frequencies would drop to zero as $k\to0$. This effect is similar to that which we have for a surface mode on a single slab of thickness d as given by Eq. (2.17). Here the frequency in the limiting case $k\to0$, $d\to\infty$ always depends on the value of the product $k\cdot d$. Physically this makes sense because neither case $k\to0$ nor $d\to\infty$ can strictly be reached in reality. Similarly for a multilayer $N\to\infty$ cannot strictly be reached and we would have to decide from the formulas derived in this section what the actual frequencies would be for some combination of a large N and a small d. The interesting aspect here is that a large N is not necessarily linked to a thick sample but can also be obtained by making the single layers thin enough.

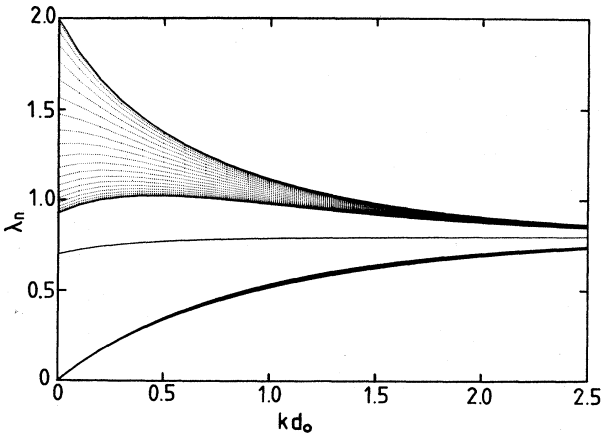

FIG. 2. Modes λ_n vs kd_0 for $N=41$ at $kd=0.5$. Shown are the two positive bands (dotted lines) and the band edges (full lines). The mode between the bands is the surface mode.

B. Case 2

ρ_1 and ρ_2 are real. Similarly as in Ref. 2, we represent E as

$$E=SRS^{-1}\ , \tag{2.18}$$

where $S=(e_1,e_2)$, e_i, $i=1,2$, are the eigenvectors of E and equal the transpose of (ξ_i,η_i), and

$$R=\begin{bmatrix}\rho_1 & 0\\ 0 & \rho_2\end{bmatrix}\ . \tag{2.19}$$

Inserting (2.18) into (2.9) we obtain

$$v_{2l+1}=\frac{1}{\xi_1\eta_2-\xi_2\eta_1}(a\rho_1^l e_1-b\rho_2^l e_2)\ , \tag{2.20}$$

with

$$\begin{aligned}a&=(\eta_2 g_1-\xi_2 h_1)\ ,\\ b&=(\eta_1 g_1-\xi_1 h_1)\ .\end{aligned} \tag{2.21}$$

Since ρ_1 and ρ_2 are real and $\rho_1\rho_2=1$, we always have $|\rho_1|>1$, $0<|\rho_2|<1$, where we choose the signs in (2.12) such that $|\rho_1|>|\rho_2|$.

If $N=2L+1$ is large such that $(\rho_2/\rho_1)^L\cong0$, Eq. (2.20) becomes

$$v_{2L+1}=\frac{a\rho_1^L}{\xi_1\eta_2-\xi_2\eta_1}e_1\ . \tag{2.22}$$

This inserted into (2.3b) yields

$$[(1+\lambda)e^{kd}\xi_1+\eta_1]a=0\ , \tag{2.23}$$

which is fulfilled if either the quantity inside the brackets, in the following denoted by [ ], equals 0 or $a=0$. In the following we assume ξ_i,η_i as in Ref. 2, i.e., $\xi_i=-e_{12}$, $\eta_i=e_{11}-\rho_i$, $i=1,2$.

(i) $a=0$. Using (2.3a) for g_1,h_1, (2.11) for e_{ij}, and (2.12) for ρ_2 we obtain, after elimination of the square root in ρ_2, the cubic polynomial

$$[f(d_0+2d)-f(d_0)]\lambda^3+[g(d_0+2d)-g(d_0)]\lambda^2-[f(d_0+2d)-2f(d_0)+f(d_0-2d)]\lambda$$
$$-[g(d_0+2d)-2g(d_0)+g(d_0-2d)]=0\ , \tag{2.24}$$

with $f(z)=\cosh(kz)$, $g(z)=\sinh(kz)$. Two of the three real roots of (2.24) satisfy $a=0$ (the third satisfies $b=0$), but only one is also contained in the spectrum of the λ_n. This is the mode which lies between the two positive bands (see Fig. 2). For $d_0=0$ it has the value

$$\lambda=\tfrac{1}{2}\coth(kd)\{[1+8\tanh^2(kd)]^{1/2}-1\}\ , \tag{2.25}$$

which becomes zero for $kd=0$.

(ii) [ ]$=0$. We now obtain (2.24) with λ replaced by $-\lambda$. This yields the mode which lies between the two negative bands (see Sec. III B).

To complete case 2, we briefly discuss the modifications for $N=2L$. According to (2.10) we multiply (2.22) with $B^{-1}A$. This yields new expressions for g_N and h_N, which must be inserted into (2.3b). Again we end up with a condition [algebraic expression]$\cdot a=0$, but now both factors lead to the same polynomial (2.24), in agreement with the fact that the positive mode between the bands is twofold degenerate for N even and large, only for smaller N, where $(\rho_2/\rho_1)^L$ is not negligible, the degeneracy is removed (see Sec. III A).

A single layer is characterized by two surfaces and hence two Damon-Eshbach (DE) surface modes. In an N-fold layer this leads to a total number of $2N$ modes, independent of how strong they are coupled. Under the restrictions we have imposed here, we can therefore be sure that we have found the complete mode spectrum. Negative values of λ and hence of the mode frequency ω are associated with a reversal in the propagation direction. This is due to the fact that in the $\exp[i(\omega t-ky)]$ term, describing plane-wave propagation along the y axis, k is always kept positive. Then a change in the sign of ω just means a reversal of the propagation direction. Here k is always positive because otherwise the solutions in the form in which they have been used to derive the set of equations (2.1) (see Ref. 2) would diverge at infinity. Hence keeping k positive, which yields $\pm\lambda$, is equivalent to making λ always positive and choosing $\pm k$, where k now has the same sign as λ previously. In the following we use both versions as is appropriate.

III. SYMMETRIES IN N-LAYER SYSTEMS WITH EVEN AND ODD N

In this section we show that characteristic differences exist in systems with an even or odd number of layers. These differences follow from certain symmetries inherent in the matrix M which describes the system.

A. Systems with an even number of layers

As an example we consider the case $N=4$. First we arrange Eqs. (2.3) and (2.5) such that (2.3a) is the first, and (2.3b) the last equation. The resulting matrix M then has the form

$$\begin{pmatrix}
1 & (1-\lambda)e^{kd} & 0 & 0 & 0 & 0 & 0 & 0\\
(1+\lambda)e^{kd} & 1 & (1-\lambda)e^{-kd_0} & e^{k(d-d_0)} & 0 & 0 & 0 & 0\\
e^{k(d-d_0)} & (1-\lambda)e^{-kd_0} & 1 & (1+\lambda)e^{kd} & 0 & 0 & 0 & 0\\
0 & 0 & (1-\lambda)e^{kd} & 1 & (1+\lambda)e^{-kd_0} & e^{k(d-d_0)} & 0 & 0\\
0 & 0 & e^{k(d-d_0)} & (1+\lambda)e^{-kd_0} & 1 & (1-\lambda)e^{kd} & 0 & 0\\
0 & 0 & 0 & 0 & (1+\lambda)e^{kd} & 1 & (1-\lambda)e^{-kd_0} & e^{k(d-d_0)}\\
0 & 0 & 0 & 0 & e^{k(d-d_0)} & (1-\lambda)e^{-kd_0} & 1 & (1+\lambda)e^{kd}\\
0 & 0 & 0 & 0 & 0 & 0 & (1-\lambda)e^{kd} & 1
\end{pmatrix}.$$

Thus the symmetry relation

$$m_{ij}=m_{2N-i+1,2N-j+1} \tag{3.1}$$

holds, and this relation is generally valid, if N is even.

Let us for simplicity consider the case $N=2$. The symmetry relation (3.1) then leads to a matrix

$$M=\begin{bmatrix} m_{11} & m_{12} & m_{13} & m_{14}\\ m_{21} & m_{22} & m_{23} & m_{24}\\ m_{24} & m_{23} & m_{22} & m_{21}\\ m_{14} & m_{13} & m_{12} & m_{11}\end{bmatrix}, \tag{3.2}$$

and the system $Mx=0$ remains unchanged, if the first and the last equation, and the second and the last but one, are added to or subtracted from each other. We obtain

$$\begin{aligned}(m_{11}\pm m_{14})(x_1\pm x_4)+(m_{12}\pm m_{13})(x_2\pm x_3)=0\ ,\\ (m_{21}\pm m_{24})(x_1\pm x_4)+(m_{22}\pm m_{23})(x_2\pm x_3)=0\ .\end{aligned} \tag{3.3}$$

The system $Mx=0$ thus decomposes into two systems $M_{\pm}x_{\pm}=0$ of size N, where $M_{+}x_{+}=0$ results from (3.3) if the upper sign is taken, and $M_{-}x_{-}=0$ follows for the lower sign.

The determinants of M_{+} and M_{-} will in general not be zero simultaneously. We therefore distinguish two cases.

(i) $|M_{-}|\neq 0$. From $x_{-}\equiv 0$ we find $x_1=x_4$ and $x_2=x_3$. The condition $|M_{+}|=0$ determines N eigenvalues λ_n.

(ii) $|M_{+}|\neq 0$. From $x_{+}\equiv 0$ we find $x_1=-x_4$ and $x_2=-x_3$. The condition $|M_{-}|=0$ determines the remaining N eigenvalues.

These results are readily generalized to arbitrary $N=2L$, and the coefficients g_l,h_l satisfy

$$\begin{aligned}g_l&=\sigma h_{2L-l+1}\ ,\\ h_l&=\sigma g_{2L-l+1}\ ,\quad \sigma=\pm 1\ ,\quad l=1,\ldots,2L\ .\end{aligned} \tag{3.4}$$

The two representations $\sigma=+1$ and $\sigma=-1$ correspond to antisymmetric and symmetric mode patterns, respectively (see below).

Figure 3(a) shows schematically the distribution of the eigenvalues with respect to the different bands, if N is even. This scheme even holds for $L=1$, i.e., the double layer, which has been treated in Ref. 7, where also mode patterns were shown. For this purpose the potential inside a magnetic layer is needed. The potential in the lth layer for mode λ_n is given by

$$\psi_l^{(n)}=(g_l^{(n)}e^{k(x-x_l)}+h_l^{(n)}e^{-k(x-x_l)})e^{-iky}\ , \tag{3.5}$$

where x and y are the coordinates introduced in Fig. 1, and x_l is the center of the lth layer. The m-field patterns follow from

$$\begin{aligned}m_x&=\frac{1}{2\pi\lambda_n}\mathrm{Im}\frac{\partial}{\partial y}\psi_l^{(n)}\ ,\\ m_y&=\frac{1}{2\pi\lambda_n}\mathrm{Im}\frac{\partial}{\partial x}\psi_l^{(n)}\ .\end{aligned} \tag{3.6}$$

[See Eq. (1) of Ref. 7 with $\kappa=0$ and $\nu=2/\lambda$.] In Fig. 4 we present some mode patterns according to (3.6) for $N=10$.

Figures 4(a) and 4(b) show the mode patterns for the largest eigenvalue of the upper and lower positive band, respectively. We observe that the upper band patterns form vortices of neighboring layers, whereas in the lower band pairs of layers exhibit an "antivortex" structure. Both patterns are antisymmetric with respect to the center plane. Figures 4(c) and (4d) show the mode patterns of the surface modes, the antisymmetric one belonging to the larger eigenvalue.

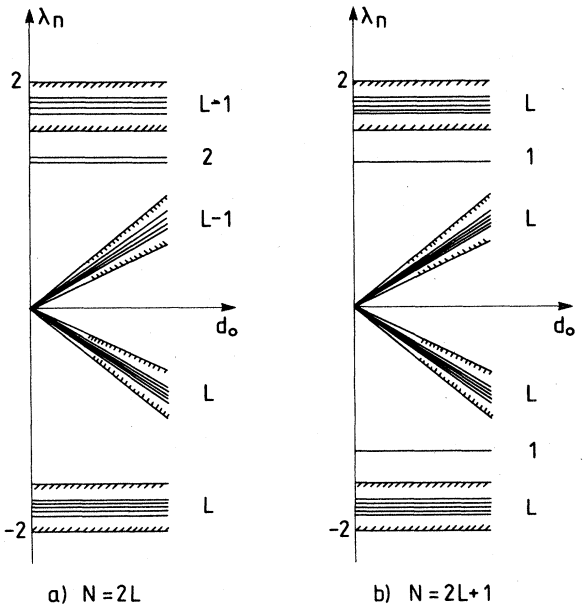

FIG. 3. Schematical distribution of the λ_n, $n=1,\ldots,2N$, vs d_0 with respect to, and between, the bands. (a) $N=2L$; (b) $N=2L+1$, for $L=5$.

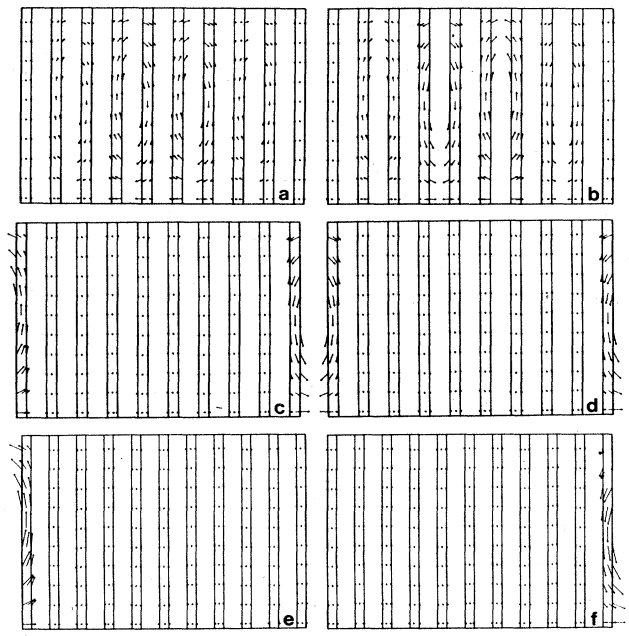

FIG. 4. Mode patterns for $N=10$. Shown is the m field at $kd=0.5$, $kd_0=1.0$ for the largest eigenvalue of the upper (a) and the lower (b) positive band. Mode patterns of the surface modes are shown in c/d, and for $N=11$ in e/f.

B. Systems with an odd number of layers

Here the simplest nontrivial case is $N=3$. Again we arrange Eqs. (2.3a) and (2.3b) as before and obtain the matrix

$$\begin{bmatrix} 1 & (1-\lambda)e^{kd} & 0 & 0 & 0 & 0 \\ (1+\lambda)e^{kd} & 1 & (1-\lambda)e^{-kd_0} & e^{k(d-d_0)} & 0 & 0 \\ e^{k(d-d_0)} & (1-\lambda)e^{-kd_0} & 1 & (1+\lambda)e^{kd} & 0 & 0 \\ 0 & 0 & (1-\lambda)e^{kd} & 1 & (1+\lambda)e^{-kd_0} & e^{k(d-d_0)} \\ 0 & 0 & e^{k(d-d_0)} & (1+\lambda)e^{-kd_0} & 1 & (1-\lambda)e^{kd} \\ 0 & 0 & 0 & 0 & (1+\lambda)e^{kd} & 1 \end{bmatrix} .$$

Now the symmetry relation

$$m_{ij}(\lambda)=m_{2N-i+1,2N-j+1}(-\lambda) \tag{3.7}$$

holds for all $N=2L+1$.

The characteristic polynomial of this generalized eigenvalue problem is

$$P_{2N}(\lambda)=\det[M(\lambda)] . \tag{3.8}$$

The determinant can be expanded into its cofactors by starting either in the upper left or, in strictly reverse order, in the lower right corner such that if

$$P_{2N}(\lambda)=f(m_{11}(\lambda),\ldots,m_{ij}(\lambda),\ldots) , \tag{3.9}$$

then also

$$P_{2N}(\lambda)=f(m_{NN}(\lambda),\ldots,m_{2N-i+1,2N-j+1}(\lambda),\ldots) , \tag{3.10}$$

where the two explicitly written arguments assume the same positions in the function $f(m_{11},\ldots,m_{NN})$. Using (3.7) we find that

$$P_{2N}(\lambda)=P_{2N}(-\lambda) , \tag{3.11}$$

i.e., if λ_n is an eigenvalue, then $-\lambda_n$ is also an eigenvalue. Figure 3(b) shows again the schematical distribution of the modes, now for $N=2L+1$.

Figures 4(e) and 4(f) show the mode patterns of the two surface modes for $N=11$, where Fig. 4(e) corresponds to the positive eigenvalue.

The results obtained in this section reveal an interesting duality between systems with even and odd numbers of layers: The symmetry properties of M are reflected in the eigenvectors if N is even, and in the eigenvalues if N is odd.

C. General symmetry considerations

As mentioned at the end of the preceding section, we find the following general symmetry properties of the antiparallel multilayer. For an even number of layers N the mode patterns turn out to be symmetric or antisymmetric with respect to a center plane (Fig. 4), but there is no apparent symmetry for the frequencies. In contrast to this, for odd N the mode patterns do not show any apparent symmetry but now the eigenvalues appear always in pairs of $\pm\lambda$.

We can attribute this to the different symmetries associated with the two kinds of multilayers. To demonstrate this we take again the simplest nontrivial cases as shown in Fig. 5. For two layers (and all other even numbers) obviously a rotation C_2^h by π around a horizontal axis, as indicated, brings the system back into itself. For three layers (representing all other odd numbers) the rotation has to be around a vertical axis (C_2^v) in order to achieve this. The important difference now is that for the modes under consideration C_2^h does not change the direction of propagation, whereas C_2^v does. Hence for the even number of layers a state described by a certain wave vector, k has to transform according to the irreducible representations of the C_2^h group which yields the properties described above. For the odd number of layers the symmetry C_2^v transforms k into $-k$, which, as stated at the end of Sec. II, is equivalent to a transformation of λ into $-\lambda$. Hence the result that if λ is an eigenvalue, $-\lambda$ is also, again is explained by symmetry.

The latter relation is also true for the "parallel" multilayer which has been treated previously. Hence independent of whether N is even or odd here we always have the $\pm\lambda$ symmetry.

However, to give a counter example one should mention that double layers consisting of films with the same magnetization but different thicknesses obviously do not have the C_2^v symmetry and yet the eigenvalues come in pairs of $\pm\lambda$.

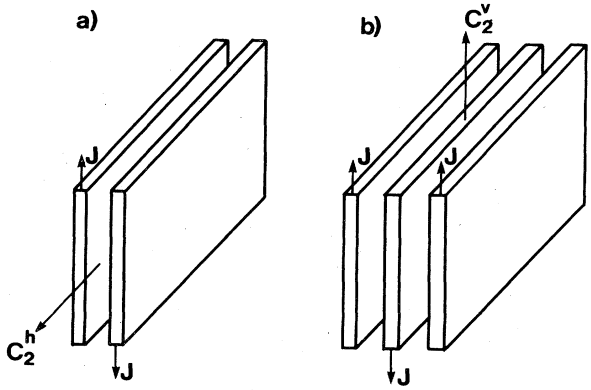

FIG. 5. Symmetry of an even- and an odd-N type of multilayer represented by (a) $N=2$ and (b) $N=3$. The symmetry is rotation about π around a horizontal axis in (a) and a vertical axis in (b).

IV. CONCLUDING REMARKS

As we have seen for large N the volume modes of an APML form two bands for each sign of λ, i.e., each propagation direction. In addition for each surface there is a surface mode. We want to compare this with the result previously obtained for an antiferromagnet[8] (AF) because an APML consisting of very thin layers has a structure similar to an AF. To underline this we consider MnO which is one of the model AF's. The Mn ions which carry the moments form an fcc lattice with the moments reversed for each pair of nearest neighbors. It turns out that the Mn ions sitting on (111) planes have their moments all parallel but they are antiparallel for neighboring planes. Here this can be regarded as an APML on an atomic scale.

Spin waves in AF's have been discussed for a long time but only recently[8] has a surface mode comparable to the DE mode on ferromagnets been predicted. Qualitatively, the result of Ref. 8 resembles the one obtained here: There are two volume mode bands and a surface mode branch in between. From elementary considerations the number of 2 for the volume modes of a simple antiferromagnet comes from the number of 2 for the magnetic moments per unit cell. Note in this context that the number of the degrees of freedom for a spin precession is only 1, in contrast to the oscillation of a single atom where it is 3. The antiferromagnetic lattice can be generated from the two moments in the unit cell by translations which correspond to the different possible k vectors. Likewise, for $N\rightarrow\infty$ the antiparallel multilayer can be generated from two antiparallel layers forming a "unit cell" by translations. Hence indeed from symmetry we expect the same number of bands. Surface modes in all cases come from the existence of surfaces and the associated boundary conditions.

As far as the interactions are concerned, our treatment of the APML and the one given in Ref. 8 for the AF are rather different. For example, we do not consider negative exchange between the layers which would correspond to the interlattice exchange interaction described in Ref. 8 in terms of molecular fields. Also we have not considered here the uniaxial anisotropy included in the theory of Ref. 8. On the other hand, the molecular field approach of Ref. 8 microscopically is only justified by isotropic nearest-neighbor exchange. Hence this approach would also have to be modified in going from an atomic layered structure like MnO to a more general one as considered here. It might be worthwhile to look into this transition in the future if further progress in preparation techniques like molecular-beam epitaxy makes the production of the related layered materials possible.

ACKNOWLEDGMENTS

We wish to thank W. Zinn for continued support and interest in this work and D. Henkel for assistance in the numerical calculations.

[1]R. E. Camley, T. S. Rahman, and D. L. Mills, Phys. Rev. B **27**, 261 (1983).
[2]P. Grünberg and K. Mika, Phys. Rev. B **27**, 2955 (1983).
[3]P. R. Emtage and M. R. Daniel, Phys. Rev. B **29**, 212 (1984).
[4]I. K. Schuller and M. Grimsditch, J. Appl. Phys. **55**, 2491 (1984).
[5]See for example, J. P. Castera, J. Appl. Phys. **55**, 2506 (1984).
[6]P. Grünberg, Proceedings of the Conference on Magnetism and Magnetic Materials [J. Appl. Phys. (to be published)].
[7]P. Grünberg, J. Appl. Phys. **52**, 6824 (1981).
[8]R. E. Camley, Phys. Rev. Lett. **45**, 283 (1980).